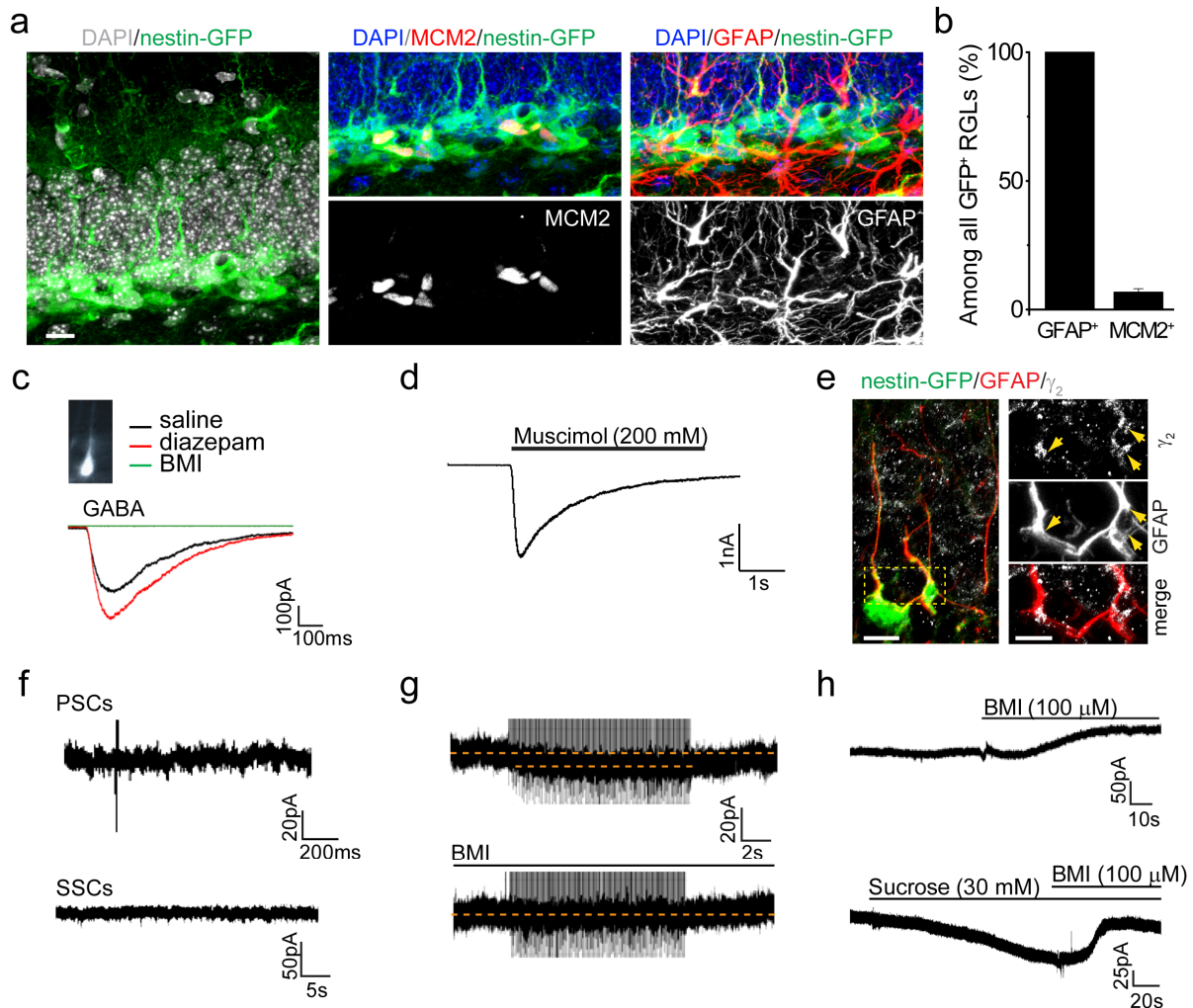
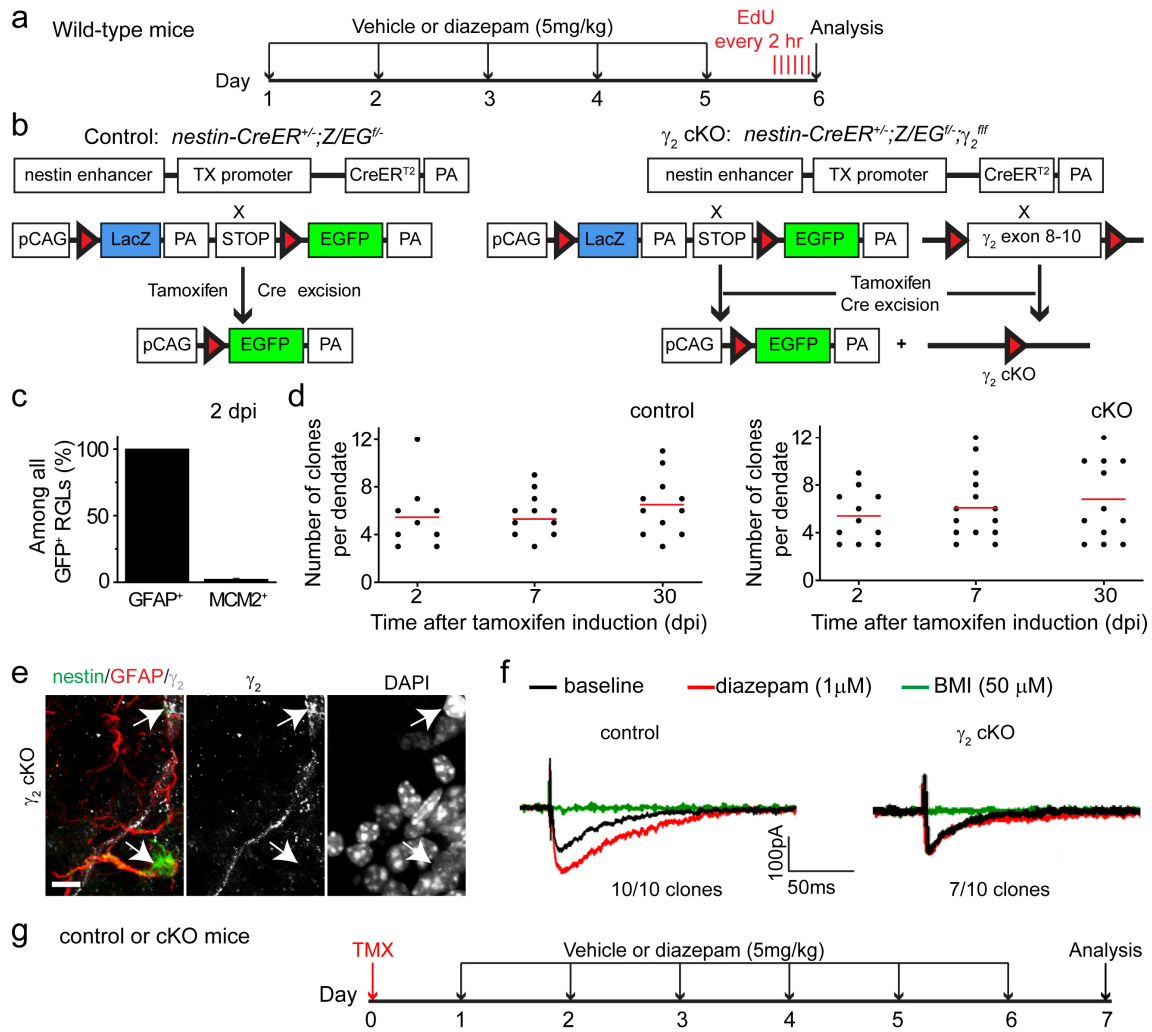


Supplementary Figures



Supplementary Figure 1. Basic characterization of GFP⁺ RGLs in the dentate gyrus of adult *nestin*-GFP mice. **a**, Sample confocal images of GFP, DAPI and immunostaining of GFAP and MCM2 in the dentate gyrus of adult *nestin*-GFP mice. Scale bar: 10 μ m. **b**, Quantification of the percentages of GFAP⁺ or MCM2⁺ RGLs among all GFP⁺ RGLs in the dentate gyrus of adult *nestin*-GFP mice. Values represent mean \pm s.e.m. (n = 3 animals). **c-h**, Sample traces of whole-cell voltage-clamp recording from GFP⁺ RGLs in slices acutely prepared from adult *nestin*-GFP mice ($V_m = -65$ mV). Shown are sample traces of a GFP⁺ RGL in response to puffs of GABA (200 mM), in the presence or absence of diazepam (1 μ M) or bicuculline (BMI; 50 μ M, **c**), and response to muscimol (200 mM, **d**). Also shown is an imaging of a recorded cell loaded with dye through the recording pipette (**c**). Shown in (**e**) are sample confocal images of GFP⁺ cells (green) immunostained for GFAP (red) and γ_2 (white) in the dentate gyrus of adult *nestin*-GFP mice. Scale bars: 10 μ m (left) and 5 μ m (right for insert). Shown in (**f**) are traces indicating a lack of evoked postsynaptic currents (PSCs) in a GFP⁺ RGL in response to the field stimulation of the dentate granule cell layer (top) and no spontaneous synaptic currents (SSCs; bottom). Shown in (**g**) are sample traces of a GFP⁺ RGL in response to a train of field stimuli (8 Hz, 100 stimuli) of the dentate granule cell layer, in the presence or absence of BMI (50 μ M). Note tonic responses induced by the stimuli. Shown in (**h**) are sample traces from a GFP⁺ RGL in response to bath application of bicuculline (BMI; 100 μ M; top), revealing the basal level of tonic responses, and from a GFP⁺ RGL in response to bath application of sucrose (30 mM) to increase the presynaptic release probability, followed by BMI treatment (bottom), demonstrating the presence of a tonic response to ambient GABA, but not synaptic GABAergic responses.



Supplementary Figure 2. Analysis of the role of γ_2 -containing GABA_ARs in regulating

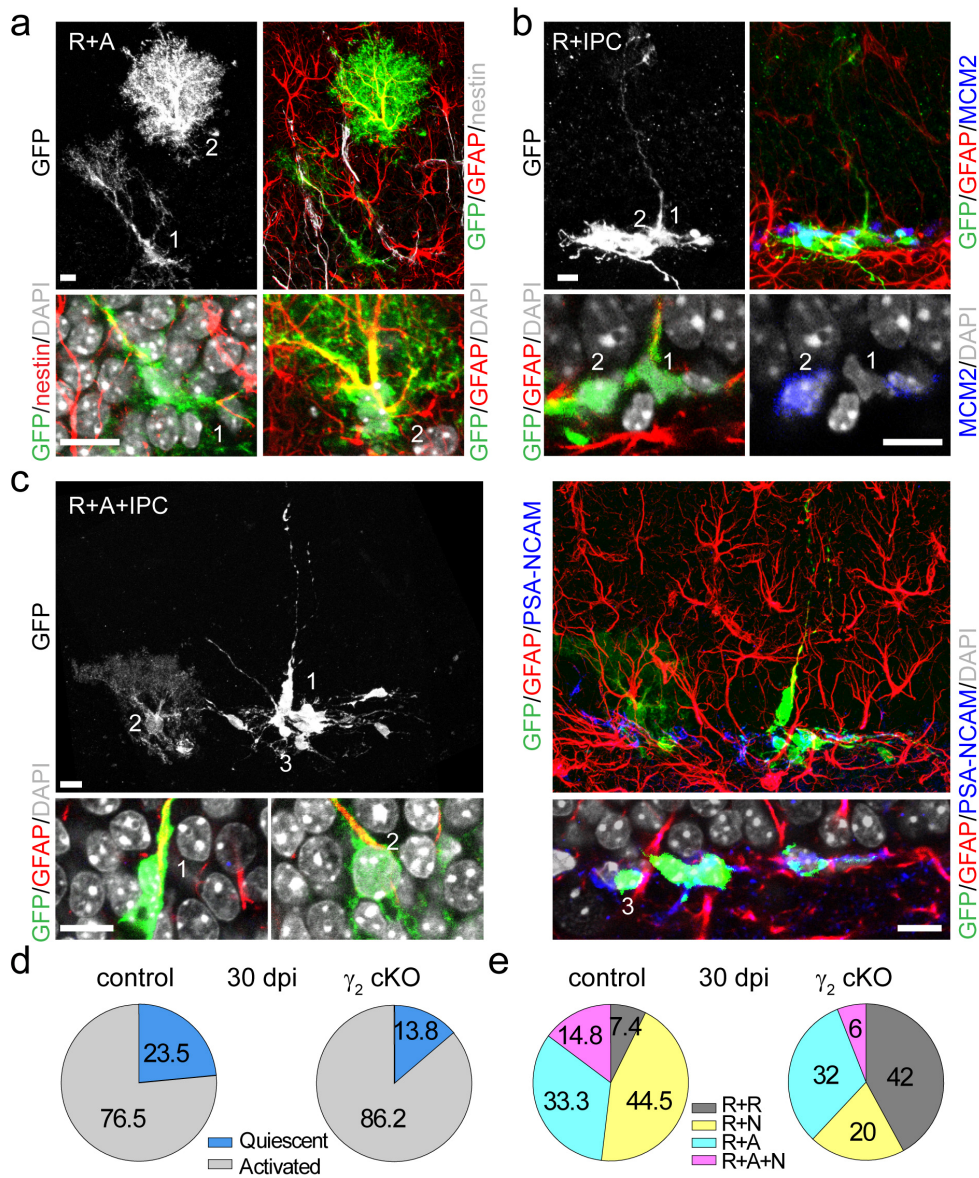
RGLs in the adult dentate gyrus. **a**, Experimental scheme for diazepam experiment (related to

Fig. 2a-b). Wild-type adult mice were *i.p.* injected with diazepam (5 mg/kg body weight; once daily for 5 days), followed by 6 injections of EdU (41.1 mg/kg body weight) at 2 hrs apart, and then processed for immunohistology 2 hrs after the last EdU injection. **b**, A schematic diagram for *in vivo* clonal analysis of individual RGLs with or without conditional γ_2 deletion. **c-d**, Basic

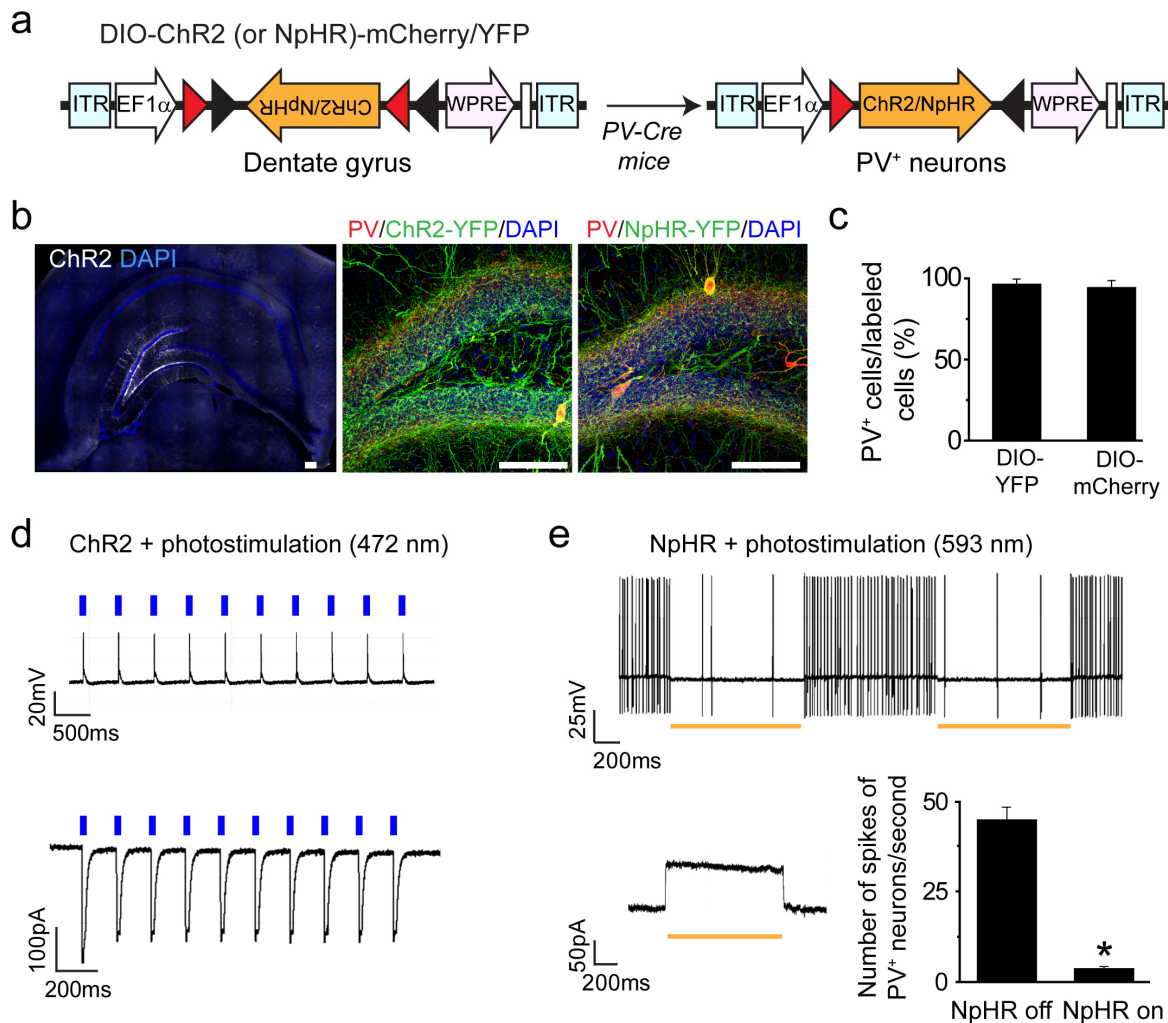
characterization of the clonal analysis approach. Shown in **(c)** is the quantification of immunohistological characterization of GFP⁺ RGLs in the subgranular zone of the adult dentate gyrus of control mice at 2 dpi. Values represent mean \pm s.e.m (n = 4-8 animals). Shown in **(d)**

are total numbers of clones in each of the dentate gyrus examined for both control and γ_2 cKO adult mice under basal conditions. Each dot represents data from one dentate gyrus. Red lines represent mean values. **e-f**, Characterization of the efficacy of γ_2 deletion in the clonal analysis. Shown in **(e)** are sample confocal images of immunostaining of GFP, GFAP and γ_2 . Scale bar: 10 μ m. Shown in **(f)** are representative whole-cell recording traces of GABAergic synaptic

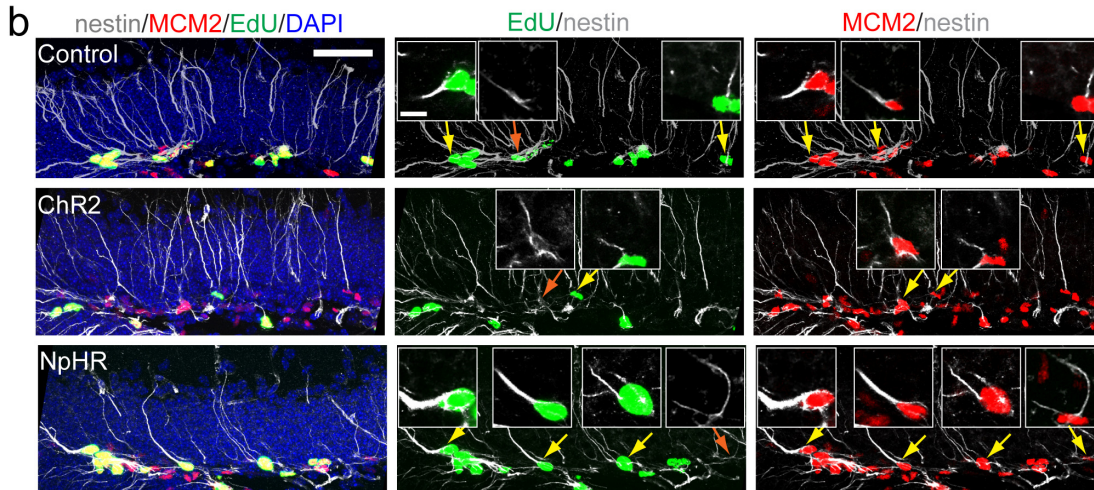
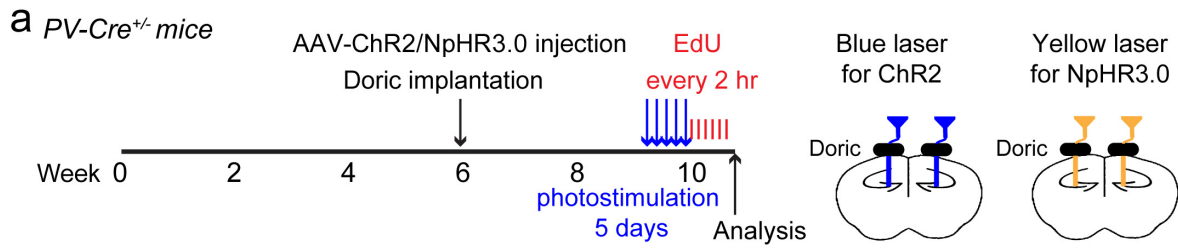
currents from GFP⁺ neurons before and after application of diazepam (1 μ M) and BMI (50 μ M) at 30 dpi in acute slices prepared from induced control and cKO mice. Numbers indicate number of clones with the phenotype among all recorded clones. **g**, A schematic diagram of experimental scheme to analyze the effect of systemic diazepam application in clonal analysis (related to **Fig. 2e & 3d**). After a single dose of tamoxifen injection (62 mg/kg body weight), vehicle or diazepam (5 mg/kg body weight) was *i.p.* injected once daily for 6 days, and animals were processed for immunohistology one day later for clonal analysis.



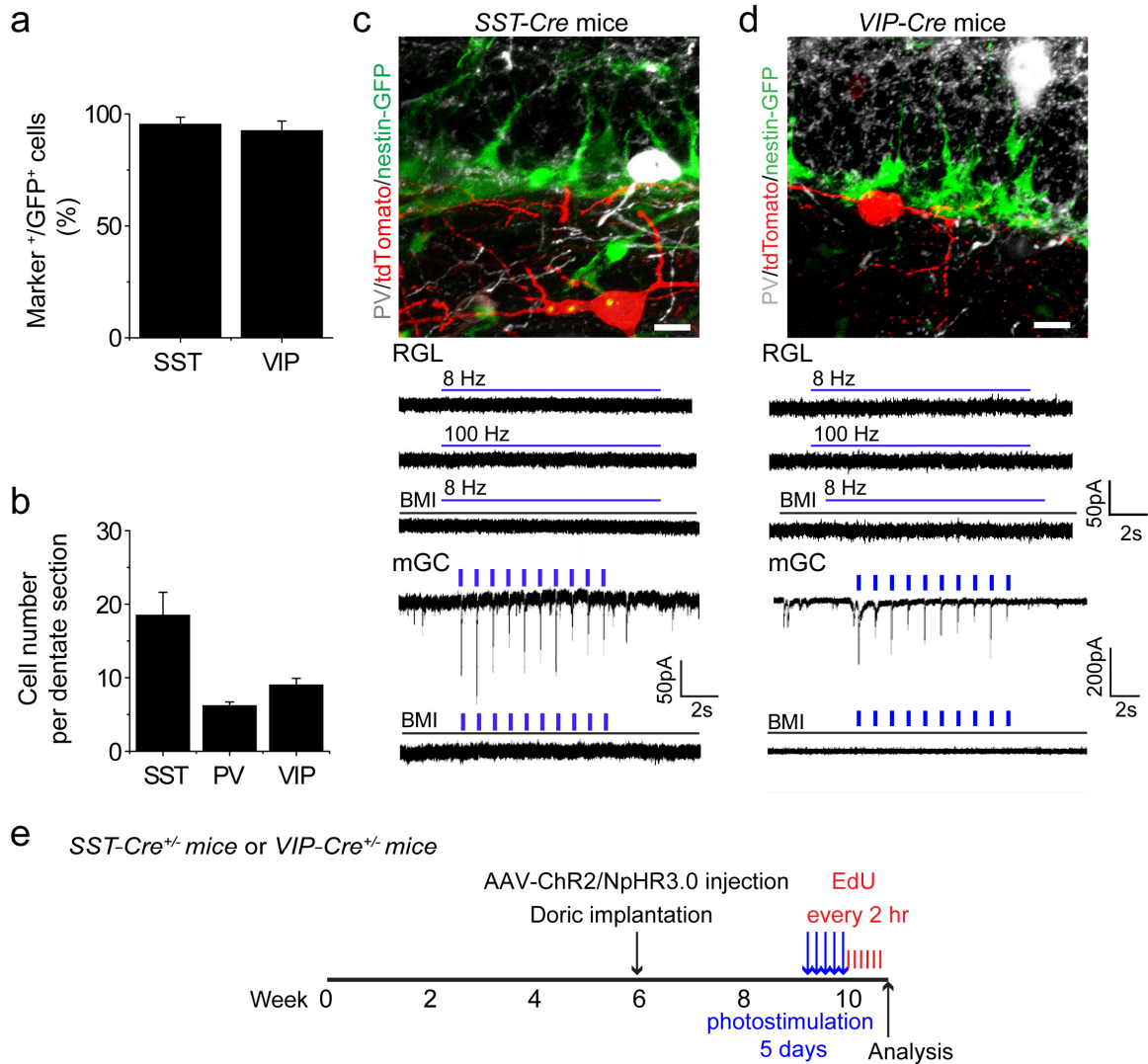
Supplementary Figure 3. Clonal analysis of γ_2 function in regulating RGLs at 30 dpi in the adult dentate gyrus. **a-c**, Sample confocal images of clones exhibiting active self-renewal. Shown in **(a)** is a GFP⁺ clone consisting of a nestin⁺GFAP⁺ RGL (1) and a nestin⁻GFAP⁺ bushy astrocyte (2), indicating self-renewal and unipotential astrogenic differentiation. Shown in **(b)** is a GFP⁺ clone consisting of a GFAP⁺MCM2⁻ RGL (1) and GFAP⁻MCM2⁺ IPCs (2), indicating self-renewal and unipotential neurogenic differentiation. Shown in **(c)** is a GFP⁺ clone consisting of a GFAP⁺ RGL (1), a GFAP⁺ bushy astrocyte (2), and a cluster of cells of the neuronal lineage (3), some of which expressed immature neuronal marker PSA-NCAM, indicating self-renewal and multi-lineage differentiation. Scale bars: 10 μ m. **d-e**, Quantitative comparison of the frequency of different clone types between control (n = 7) and γ_2 cKO (n = 6) at 30 dpi. Shown are pie charts of the relative frequency of quiescence/activation (**d**) and the summary of the frequency of different types among all RGL-containing GFP⁺ clones (**e**).



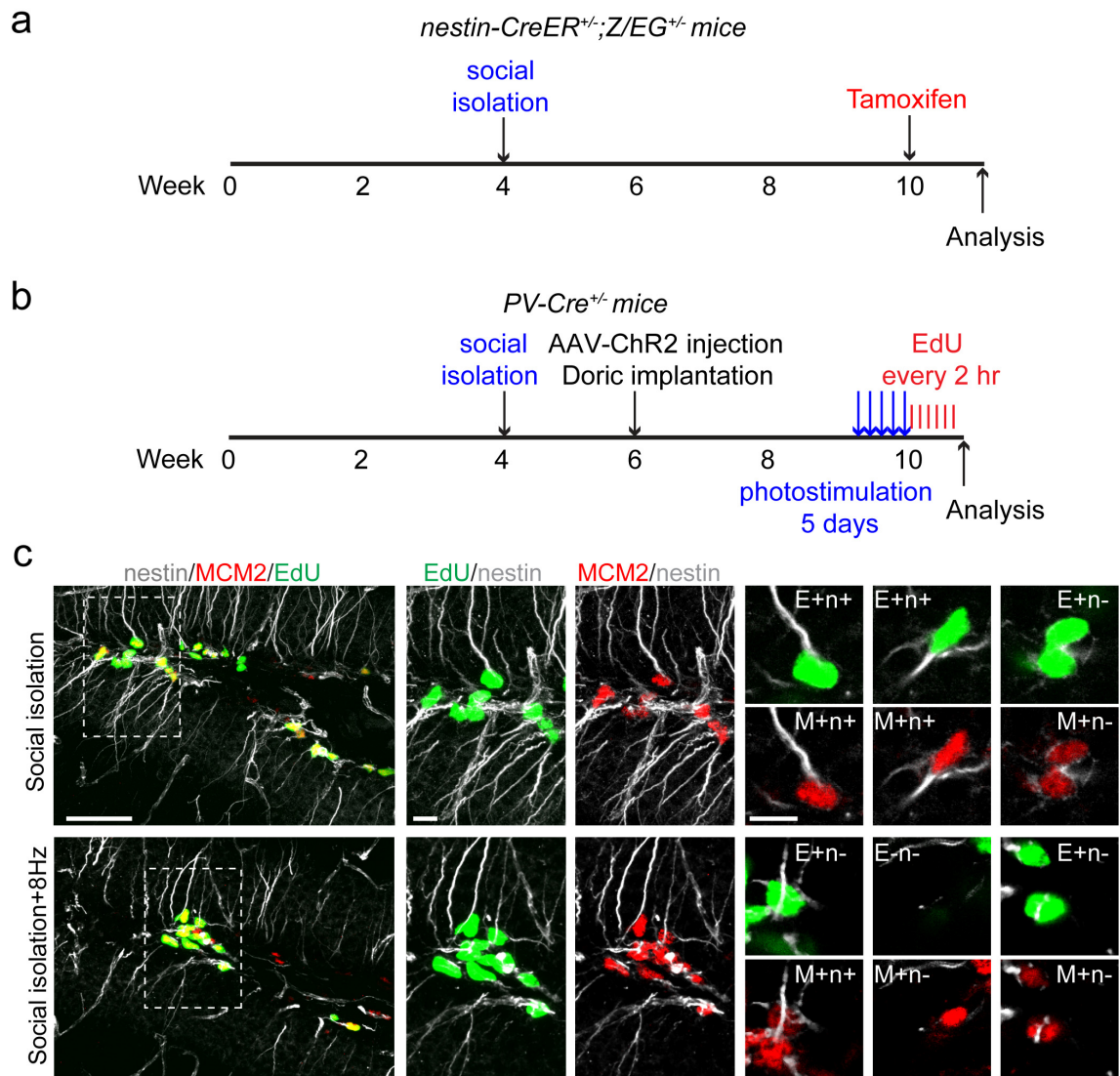
Supplementary Figure 4. Characterization of optogenetic tools for manipulating PV⁺ interneuron activity in the adult dentate gyrus. **a**, A schematic diagram of AAV constructs used for Cre-dependent expression of ChR2 or eNpHR in PV⁺ interneurons using adult *PV-Cre* mice. **b**, Sample confocal images of expression of ChR2-YFP or eNpHR-YFP and PV immunostaining 2 weeks after AAV-DIO-ChR2-YFP or AAV-DIO-NpHR-YFP injection into the dentate gyrus of adult *PV-Cre* transgenic mice. Scale bars: 50 μ m. **c**, Quantification of the specificity of AAV-mediated expression in PV⁺ interneurons in the adult dentate gyrus. Shown are summaries for both YFP and mCherry tagged opsin vectors ($n = 5-10$ animals). **d-e**, Effective photo-activation or suppression of PV⁺ interneurons in slices acutely prepared from AAV injected animals. Shown are sample traces of whole-cell recordings of YFP⁺PV⁺ interneurons under both current-clamp (upper traces) and voltage-clamp modes (lower traces) upon photo-activation (**d**; 472 nm blue light at 8 Hz, 5 ms) or upon photo-suppression (**e**; 593 nm yellow light; constant). Also shown is the quantification of the efficiency of photo-induced suppression. A current pulse of 100 pA current was delivered to YFP⁺PV⁺ interneurons, and the number of action potentials with or without yellow light on was quantified. Values represent mean \pm s.e.m. ($n = 6$ cells; *: $P < 0.05$; student t-test).



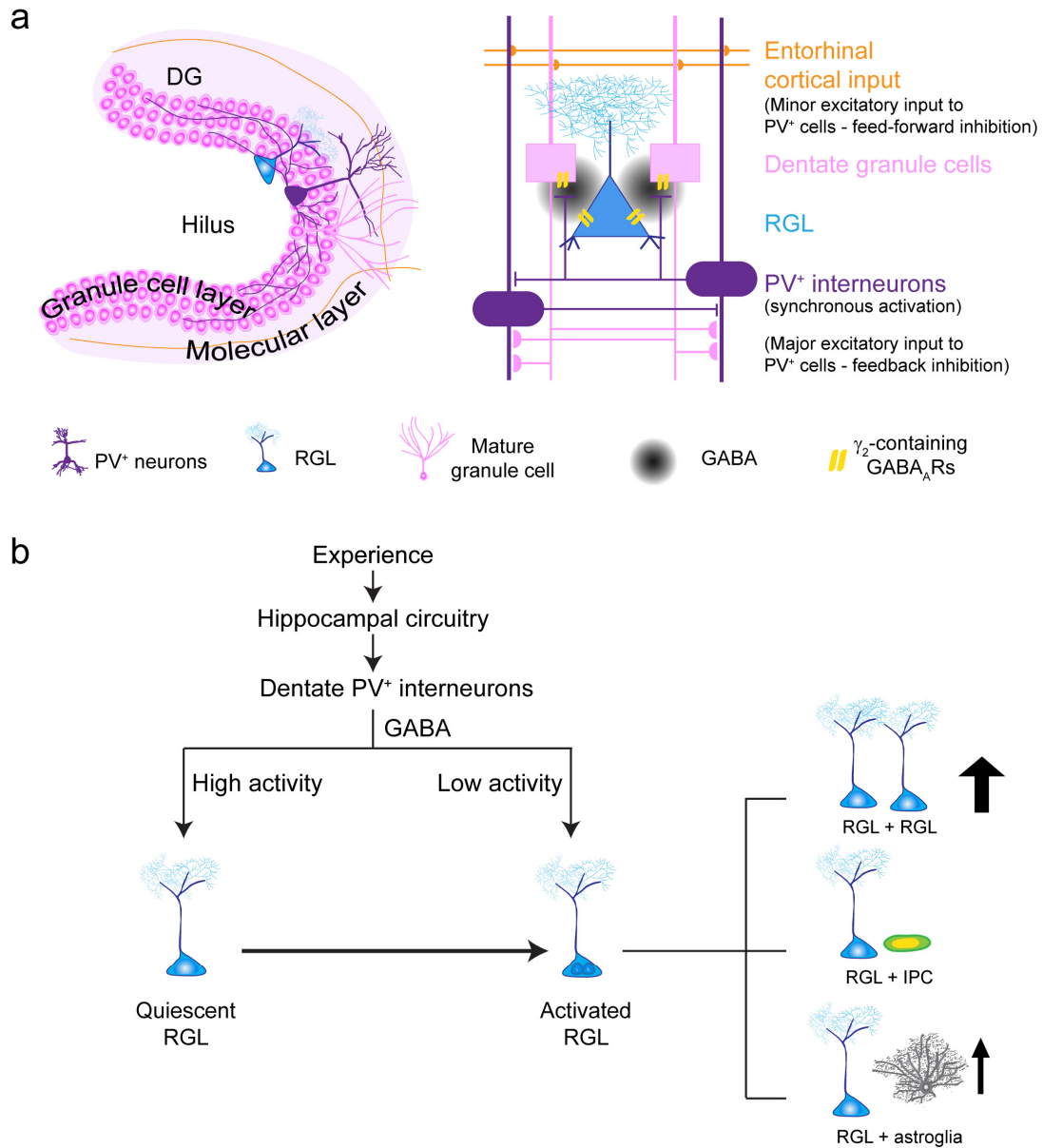
Supplementary Figure 5. Analysis of effects of *in vivo* manipulation of PV⁺ interneuron activity on RGL activation in the adult dentate gyrus of *PV-Cre* mice. **a**, A schematic diagram of analysis of RGL activation at the population level upon photo-activation or photo-suppression of PV⁺ interneurons in the dentate gyrus of adult *PV-Cre* mice (related to **Fig. 4d**). For photo-activation of PV⁺ interneurons, blue light flashes (472 nm; 5 ms at 8 Hz) were delivered every 5 minutes for 30s/per trial, 8 hrs per day for 5 days. For photo-suppression of PV⁺ interneurons, continuous yellow light (593 nm; constant) was delivered 8 hrs per day for 5 days. On the 5th day, animals were *i.p.* injected with EdU (41.1 mg/kg body weight) 6 times 2 hrs apart and processed for immunohistology 2 hrs after the last EdU injection. **b**, Sample confocal images of immunostaining of nestin (white), MCM2 (red), EdU (green) and DAPI (blue). Yellow arrows point to double labelled RGLs (nestin⁺MCM2⁺ or nestin⁺EdU⁺ cells with radial process) and orange arrows point to EdU⁻ or MCM2⁻ nestin⁺ cells. Scale bars: 50 μm and 10 μm (insert).



Supplementary Figure 6. Characterization of optogenetic tools for manipulating SST⁺ and VIP⁺ interneuron activity in the adult dentate gyrus. **a-b**, Characterization of opsin expression in different animal models. Shown in **(a)** is a quantification of immunohistological analysis of the specificity of ChR2 expression in SST⁺ and VIP⁺ interneurons after AAV-DIO-ChR2-YFP injection into the dentate gyrus of adult SST-Cre or VIP-Cre mice, respectively. Shown in **(b)** is a summary of quantification of numbers of ChR2-YFP labelled neurons after AAV-DIO-ChR2-YFP injection into the dentate gyrus of adult PV-Cre, SST-Cre or VIP-Cre mice. Values represent mean \pm s.e.m. ($n = 3-10$ animals). **c**, Lack of responses of RGLs to SST⁺ interneuron activation. Shown at the top is a sample confocal image of nestin-GFP, ChR2-tdTomato, and PV immunostaining in the dentate gyrus of adult SST-Cre^{+/+}nestin-GFP^{+/+} mice after AAV-DIO-ChR2-tdTomato injection. Scale bar: 10 μ m. Shown at the bottom are sample whole-cell voltage-clamp recording traces from a GFP⁺ RGL upon light stimulation of SST⁺ neurons (472 nm blue light at 8 or 100 Hz) and from a mature dentate granule cell (mGC; at 1 Hz) upon light stimulation of SST⁺ interneurons in the acute slices before and after bicuculline treatment (BMI; 50 μ M). **d**, Lack of responses of RGLs to VIP⁺ interneuron activation. Similar as in **(c)**, except adult VIP-Cre^{+/+}nestin-GFP^{+/+} mice were used. **e**, A schematic diagram of analysis of RGL activation at the population level upon photo-activation or photo-suppression of SST⁺ or VIP⁺ interneurons in the adult dentate gyrus. The same paradigm as in Supplementary Fig. 5a was used.



Supplementary Figure 7. Experimental schemes involving social isolation. **a**, A schematic diagram of clonal analysis of RGLs upon social isolation (related to **Fig. 5a-b**). **b**, A schematic diagram of analysis of RGL activation at the population level upon photo-stimulation of PV⁺ interneurons in the adult dentate gyrus following social isolation (relate to **Fig. 5c**). Same paradigm of photo-stimulation and EdU injections as in Supplementary Fig. 5a was used. **c**, Sample confocal images of immunostaining for nestin (white; n), MCM2 (red; M), and EdU (green; E). Scale bars: 50 μ m (left column) and 10 μ m for inserts (five right columns).



Supplementary Figure 8. A summary model of regulation of quiescent adult neural stem cells *in vivo* in response to neuronal activity and experience, involving GABA release from local PV⁺ interneurons and γ_2 -containing GABA_AR-mediated signalling in RGLs in the adult dentate gyrus. **a, Schematic diagrams of local dentate gyrus circuitry. PV⁺ interneurons receive excitatory inputs from both dentate granule cells (90%) and entorhinal cortical inputs (5%). PV⁺ interneurons are also coupled with each other and fire synchronously. PV⁺ interneurons innervate dentate granule cell layer and spillover of GABA from synaptic junctions regulates nearby radial glia-like neural stem cells (RGLs). **b**, A model of neuronal activity-dependent regulation of radial glia-like neural stem cell fate decision in the adult dentate gyrus. High levels of PV⁺ interneuron activity promote quiescence of neural stem cells, whereas low levels of PV⁺ interneuron activity promote activation of neural stem cells and symmetric cell division.**

Supplementary Movies

Supplementary Movie 1. Close association between GFP⁺ RGLs and GAD67⁺ terminals of PV⁺ interneurons in the adult dentate gyrus. Shown is a surface-rendered reconstruction of confocal images of the dentate gyrus (90 x 90 x 30 μ m) of adult *nestin-GFP* mice for immunostaining of nestin-GFP (green), PV⁺GAD67⁺ (blue) and PV⁻GAD67⁺ (red).

Supplementary Movie 2. Lack of interaction between SST⁺ interneurons and RGLs in the adult dentate gyrus. Shown is a surface-rendered reconstruction of confocal images of PV immunostaining (white), ChR2-tdTomato expression by SST⁺ interneurons (red) and nestin-GFP expression in RGLs (green). DIO-ChR2-mCherry AAV was injected into *SST-Cre^{+/+};nestin-GFP^{+/+}* mice and sections were processed for immunostaining two weeks later. Note that SST⁺ interneurons extend neuronal processes in the subgranular zone and hilus region, whereas PV⁺ interneurons exhibit elaborated processes in the subgranular zone and granule cell layer in the adult dentate gyrus.

Supplementary Movie 3. A single PV⁺ interneuron has the capacity to regulate a large number of RGLs in the adult dentate gyrus. Shown is a surface reconstruction of serial confocal images of a single PV⁺ interneuron in the adult dentate gyrus. A small volume of DIO-mCherry AAV was injected into *PV-Cre^{+/+};nestin-GFP^{+/+}* mice and a region with a single PV⁺ neuron was confocal imaged for mCherry (PV⁺ neuron) and GFP (nestin-expressing cells) 2 weeks after injection and reconstructed from 8 serial coronal sections (50 μ m in thickness per section). An estimated 200+ GFP⁺ RGLs were covered by a single PV⁺ interneuron in the adult dentate gyrus.